Structure and energetics of hydroxylated silica clusters, (SiO2)M(H2O)N, M=8,16 and N=1-4: A global optimisation study

Flikkema, Edwin; Jelfs, Kim E.; Bromley, Stefan T.

Published in:
Chemical Physics Letters

DOI:
10.1016/j.cplett.2012.10.016

Publication date:
2012

Citation for published version (APA):
Flikkema, E., Jelfs, K. E., & Bromley, S. T. (2012). Structure and energetics of hydroxylated silica clusters, (SiO2)M(H2O)N, M=8,16 and N=1-4: A global optimisation study. *Chemical Physics Letters*, *554*, 117-122. https://doi.org/10.1016/j.cplett.2012.10.016

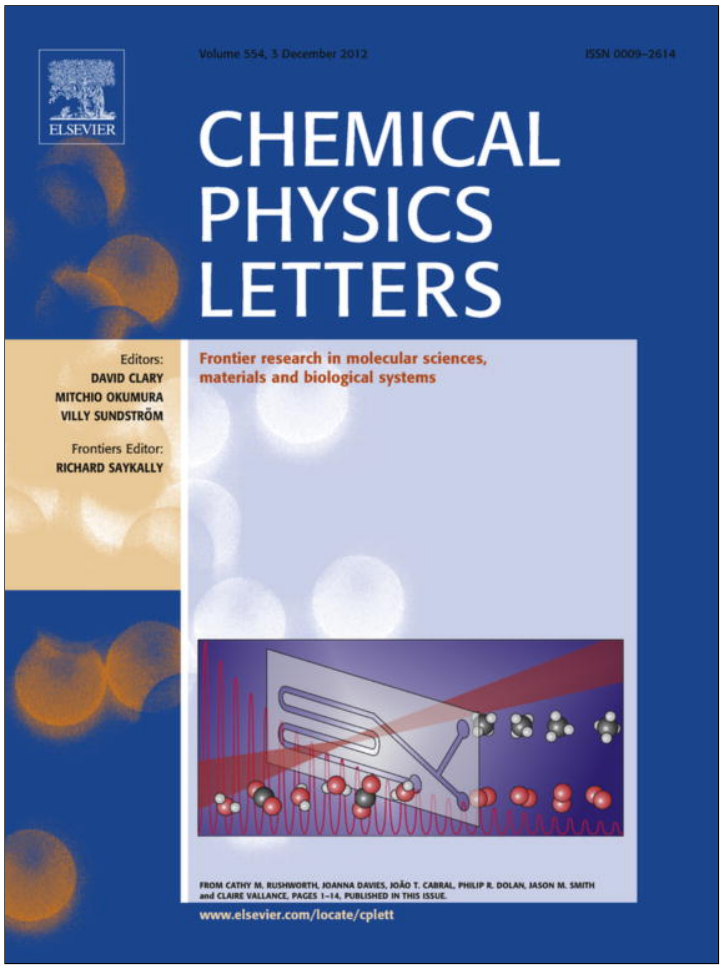

Chemical Physics Letters 554 (2012) 117–122

Contents lists available at SciVerse ScienceDirect

Chemical Physics Letters

journal homepage: www.elsevier.com/locate/cplett

Structure and energetics of hydroxylated silica clusters, $(SiO_2)_M(H_2O)_N$, $M = 8$, 16 and $N = 1 - 4$: A global optimisation study

Edwin Flikkema [a,*], Kim E. Jelfs [b], Stefan T. Bromley [c,d,*]

[a] Institute of Mathematics and Physics, Aberystwyth University, Penglais, Aberystwyth, Ceredigion SY23 3BZ, United Kingdom
[b] Department of Chemistry, University of Liverpool, Crown Street, Liverpool L69 7ZD, United Kingdom
[c] Departament de Quimica Fisica & Institut de Quimica Teorica i Computacional, Universitat de Barcelona, Marti i Franques 1, E-08028 Barcelona, Spain
[d] Institucio Catalana de Recerca i Estudis Avancats (ICREA), E-08010 Barcelona, Spain

ARTICLE INFO

Article history:
Received 1 August 2012
In final form 5 October 2012
Available online 13 October 2012

ABSTRACT

The low energy isomer spectrum of hydroxylated silica clusters, $(SiO_2)_M(H_2O)_N$, is investigated using global optimisation with an empirical potential and *ab initio* structural and energetic refinement. The cases $M = 8$, 16 and $N = 1 - 4$ are considered in gas phase with respect to their relative energetic stabilities, reaction energies (relative to hydroxylation and condensation) and geometries. All hydroxylation reactions and condensation reactions are found to be energetically downhill, with the former becoming progressively less favourable with increasing hydroxylation. Hydroxylation also appears to affect the structures of smaller anhydrous clusters more than larger ones.

1. Introduction

Silica (SiO_2) is a versatile material with many applications in optics, chemistry (catalysis/separation) and electronics. To a large extent the usefulness of silica is linked to its rich polymorphism in bulk form, ranging from the dense phases such as quartz to lower-density nanoporous phases known as zeolites. For the majority of bulk silica materials, each silicon atom is bonded to four oxygen atoms, while each oxygen atom is bonded to two silicon atoms. Often, thus, bulk silica can be regarded as an infinite network of corner-sharing tetrahedra, where the centre of each tetrahedron represents a silicon atom and the corners represent oxygen atoms. Conversely, due to their finite size, even the most energetically stable clusters of silica are expected to display non-bulk structures and exhibit terminating defects. Earlier computational studies of low energy anhydrous silica clusters using global optimisation [1–3] have indeed predicted the occurrence of many types of cluster structures and surface defects (e.g. edge-sharing tetrahedra – two-rings, terminal oxygens bound to three-coordinated silicon atoms – silanones). These defects are generally expected to be highly reactive, in particular with water, giving rise to hydroxylated silica clusters. Such small hydrated clusters of silica are important to understand due to their relevance to geology (e.g. mineral dissolution) and the synthesis of zeolites. Previous theoretical work has mainly concentrated on the latter and studied a range of small (typically $\leqslant 8$ SiO_2units) hand-selected highly hydroxylated species [4–8]. Here, we report on a systematic investigation into the gradual hydroxylation of $(SiO_2)_8$ and $(SiO_2)_{16}$ from their fully anhydrous state up to the addition of four water molecules. For both sizes and for each degree of hydroxylation our global optimisation approach (see below) allows us to provide the likely most energetically stable isomers. The choice of the $(SiO_2)_8$-based clusters is motivated by their relevance in the low hydroxylated regime as magic clusters in cluster beams [9–11] and, at a higher degree of hydroxylation, their use as possible building blocks in zeolite hydrothermal synthesis [12–14]. The systematic exploration of the initial hydroxylation of $(SiO_2)_{16}$ allows us to the compare trends for this relatively large species with the analogous process for $(SiO_2)_8$. Further, it allows us to consider the energetics of a range of $(SiO_2)_8$-based cluster condensation reactions for low $(SiO_2)_{16}$ hydroxylations, as we have recently studied for solvated species in the highly hydroxylated range [15].

2. Methodology

The Potential Energy Surface (PES) of a chemical system is defined as the energy of the system as a function of the coordinates of the atoms that make up the system. A stationary point on the PES is a point where the gradient of the energy vanishes, i.e. there is no net force acting on any of the particles. A local minimum is an example of a stationary point corresponding to a meta-stable arrangement of atoms. Only in the case of the global minimum (i.e. the minimum with the lowest energy) is the system truly stable. At low temperatures, the global minimum is the most likely state of the system to occur. This Letter focuses on locating the low-lying minima (including the global minima) on the PES of

* Corresponding author. Fax: +44 1970 622826.
E-mail addresses: edf@aber.ac.uk (E. Flikkema), K.Jelfs@liverpool.ac.uk (K. Jelfs), s.bromley@ub.edu (S.T. Bromley).

0009-2614/$ - see front matter © 2012 Elsevier B.V. All rights reserved.
http://dx.doi.org/10.1016/j.cplett.2012.10.016

hydroxylated silica clusters $(SiO_2)_M(H_2O)_N$ for $M = 8$, 16 and $N = 1 - 4$.

The energy of a system of interacting atoms and/or ions (as a function of the atomic coordinates) can be obtained using various methods with a range of accuracies, with a typical trade-off between a method's accuracy and efficiency. Electronic structure methods such as Density Functional Theory (DFT) form a relatively accurate but computationally expensive means of determining the energy. There are electronic structure methods that are more accurate (and considerably more computationally demanding) than DFT, but these will not be considered in this Letter. Empirical interatomic potentials form a simplified picture of a chemical system where the detailed description of the electrons is avoided. The system is regarded as a collection of ions and/or atoms that interact via a potential or force-field. Such a potential usually consists of two-body contributions (i.e. acting between pairs of atoms) although in some cases many-body contributions are also included, such as three-body terms.

An example of an empirical potential, which will be used in this work, is shown below,

$$U = \sum_{i<j} V_{ij}(r_{ij})$$

$$V_{ij}(r_{ij}) = \frac{q_i q_j}{4\pi\epsilon_0 r_{ij}} + A_{ij}\exp\left(-\frac{r_{ij}}{B_{ij}}\right) - \frac{C_{ij}}{r_{ij}^6} \quad (1)$$

The total system energy U is a sum which runs over all atom pairs. The potential between every atom pair, V_{ij}, is purely of two-body form, where r_{ij} corresponds to the distance between atom i and atom j. The first term of V_{ij} represents the electrostatic interaction. The charges q_i and q_j also depend on the chemical identity of the atoms i and j. These charges are typically effective fitted charges, which are not necessarily equal to the formal charge of the atom involved. The last two terms combined form a Buckingham potential, which consists of a short-range repulsive term and a longer range attractive dispersion term. The parameters A_{ij}, B_{ij} and C_{ij} depend on the chemical identity of the two atoms i and j involved. Potentials of this simple form have been successfully used to model bulk silica, with two parameterisations known as the TTAM [16] and BKS [17] potentials, being popular. These potentials take the same mathematical form as (1) and only differ in the value of the parameters q_{Si}, q_O, A_{SiSi}, A_{SiO}, A_{OO}, B_{SiSi}, B_{SiO}, B_{OO}, C_{SiSi}, C_{SiO} and C_{OO}.

The TTAM and BKS potentials have been specifically parameterised for silica in its bulk form where all Si centres are 4-coordinated. In an earlier paper we have introduced another parameterisation specifically for anhydrous nano-scale silica clusters [18] to better take into account terminating defects (e.g. silanones). In order to treat hydroxylated silica, Hassanali and Singer (HS) used the BKS silica paramerisation as base and added further two-body terms to model the interaction of silica with hydrogen and three-body terms to deal with the directionality of dangling hydroxyls (Si–O–H) [19]. In this study, where all Si centres in the reported isomers were always found to be 4-coordinated, we employ the consistent hydroxylated silica HS parameterisation. For reasons of simplicity and computational efficiency, however, we omit the three-body terms. We refer to this simplified potential as the HS_{simp} potential hereafter. One implication of the use of the HS_{simp} potential is that our initial unrefined low energy hydroxylated cluster structures do not incorporate explicit intra-cluster H-bonding. Although the positions on the clusters of the OH groups can be energetically assessed by the HS_{simp} potential, the small energy differences between local minima only differing in the orientation of the hydroxyl units cannot. Such 'orientational' isomers, which for the purposes of this study are considered to be alternative realisations of the same cluster, are thus only distinguished upon refinement at higher computational levels of theory (see below).

Once having a method to evaluate cluster energies, the problem of *local* optimisation (i.e. trying to find a nearby minimum starting from a point in coordinate space) is relatively straightforward. Local optimisation methods are usually iterative, where a new point in coordinate space is calculated on the basis of the value of the energy, the gradient and possibly the Hessian for the points that have been visited previously. Effective local optimisation methods, such as the Newton–Raphson method, require the evaluation of the Hessian. Since calculating the Hessian can be costly, quasi-Newton methods have been developed, which do not require the explicit calculation of the Hessian, but instead build an approximation to the (inverse) Hessian using gradient information from previous steps. An example of a quasi-Newton method is the L-BFGS method [20], which is used in the present study.

By comparison, for many physically realistic systems, locating the *global* minimum is a much more difficult process. For globally optimising small clusters many approaches have been suggested, ranging from genetic/evolutionary algorithms to simulated annealing [21,22]. In this Letter the Basin Hopping (BH) global optimisation method [23] is used, which we have used successfully before for anhydrous and hydrated silica clusters [1,2,10,15,24].

The Basin Hopping method is based on the Metropolis Monte Carlo (MC) method, with the added feature of a local optimisation at each step. In ordinary Metropolis MC simulation, at each step, the coordinates are changed (a MC 'move') and the energy of the changed system is compared to the energy from the previous step. If the energy goes down, the changed coordinates are accepted as the new set of coordinates. If the energy goes up, the change is accepted with a probability equal to the ratio of Boltzmann factors:

$$p_{acc} = \exp\left(-\frac{E_{cur} - E_{prev}}{kT}\right) \quad (2)$$

where E_{cur} is the energy of the current (changed) system, while E_{prev} is the energy from the previous step. The change is rejected with a probability of $1 - p_{acc}$, in which case the search process reverts back to the coordinates from the previous step. This decision process, known as the Metropolis criterion, is designed in such a way that Boltzmann statistics is achieved (provided the Monte Carlo moves are balanced and ergodic).

The BH method differs from ordinary Metropolis MC sampling in that, at each step, a local optimisation is performed, using the changed set of coordinates as a starting point. When deciding whether to accept or reject the changed coordinates, the *optimised* energies of the current and previous step are used. In this way, instead of sampling the original PES, a simplified energy surface is sampled, which is a step function, the optimised energy being constant on the basin of attraction of a certain (local) minimum. This modification of the PES improves the sampling efficiency, as barriers between neighbouring minima are removed.

In our BH runs various values of the BH parameters (mainly temperature and stepsize) were tried and various starting geometries were chosen in order to ensure good sampling. Typically an individual BH run consisted of one million steps. Initially, runs were performed at a high temperature to produce likely starting structures for subsequent runs. These (longer) runs were performed at intermediate temperatures. Finally some low energy geometries were selected as starting points for low temperature runs to scan the PES more thoroughly around each candidate ground state.

Initial low energy minima were thus generated by a combination of BH and the HS_{simp} potential. An essential part of our full methodology is, however, to take the results of this procedure only as a rough guide in generating candidates for low energy minima. As mentioned above, an obvious shortcoming of the HS_{simp} potential is that, although computationally very efficient, it leads to

unrealistic Si–O–H angles for the hydroxyl units (typically straight (180°) Si–O–H angles). To remedy this effect, intermediate optimisations using the PM3 semi-empirical method [25] were used to obtain isomers with more realistic angles and to help find the optimal intra-cluster Si–O–H orientations for each structurally distinct isomer. Promising low-energy geometries from the semi-empirical optimisations were finally optimised using Density Functional Theory (DFT). Here we use the B3LYP functional [26] and a 6-31G** basis set and no symmetry constraints using the GAMESS-UK code [27], as in our previous studies of hydroxylated silica clusters [10,15]. Up to 20 geometries were energy minimised using DFT for each of the eight cluster compositions considered. We note that, as expected, the energetic ordering of the minima, as ranked by their energy calculated via DFT, often differs from the ordering as predicted by the empirical potential due to the limited accuracy of the HS_{simp} potential.

3. Results and discussion

Our BH/HS_{simp} searches followed by higher level optimisation, produced extensive databases of cluster geometries. Below we report the structures and energetics of the eight different cluster compositions considered: $(SiO_2)_M(H_2O)_N$ with $M = 8$, 16 and $N = 1$, 2, 3, 4.

Although there is no guarantee that our procedure finds the global energetic minimum, we take the lowest minimum found for each composition as the best candidate for the global minimum. The lowest energy DFT-optimised geometries have been ranked according to their total energy and the three lowest energy geometries are shown (for each level of hydroxylation $N = 1$, 2, 3, 4) in Figure 1 (Si_8O_{16}-based clusters) and in Figure 2 ($Si_{16}O_{32}$-based clusters).

As mentioned above, the energetic ordering of the minima according to DFT may differ from the ordering according to the HS_{simp} potential. In Table 1 the DFT calculated energetic ordering and the energetic ordering according to the HS_{simp} potential are compared, both for $(SiO_2)_8(H_2O)_N$ and for $(SiO_2)_{16}(H_2O)_N$ clusters. The columns labelled 1, 2, 3 correspond to the lowest (global minima), second lowest and third lowest DFT energy minima. The entries in these columns show where these clusters are placed in the energetic ordering according to the HS_{simp} potential. Although the agreement is not perfect, the predictions of the HS_{simp} potential are fairly reliable. In half of the cases the lowest energy cluster according to the potential is also the lowest in energy according to DFT. With regards to finding the global minimum according to DFT, the worst case is $(SiO_2)_{16}(H_2O)_4$ ($M = 16$, $N = 4$) where it is the seventh lowest minimum according to the HS_{simp} potential that turns out to be the lowest energy cluster according to DFT.

Most of the isomer geometries optimised with DFT follow the conventional rules of bulk silica chemistry where silicon atoms are coordinated by four oxygen atoms and oxygen atoms are either 'bridging oxygens' (i.e. forming a bridge between two silicon atoms) or are part of a hydroxyl group. However, there are exceptions, especially for the Si_8O_{16} based clusters at low levels of hydroxylation. For example, the $(SiO_2)_8(H_2O)$ cluster geometries include 4-fold coordinated oxygen atoms and dangling oxygens. The $(SiO_2)_8(H_2O)_2$ cluster geometries include 3-fold coordinated oxygen atoms and dangling oxygens. Similar types of defects have been found in earlier studies of (hydroxylated) silica clusters and surfaces [1,2,10,28].

It is useful to compare the total energy $E_{M,N}$ of a hydroxylated silica cluster to the energy $E_{M,0}$ of the anhydrous (i.e. pure silica) cluster combined with the appropriate number of H_2O molecules:

$$\Delta_h E = E_{M,N} - (E_{M,0} + N \cdot E(H_2O)) \tag{3}$$

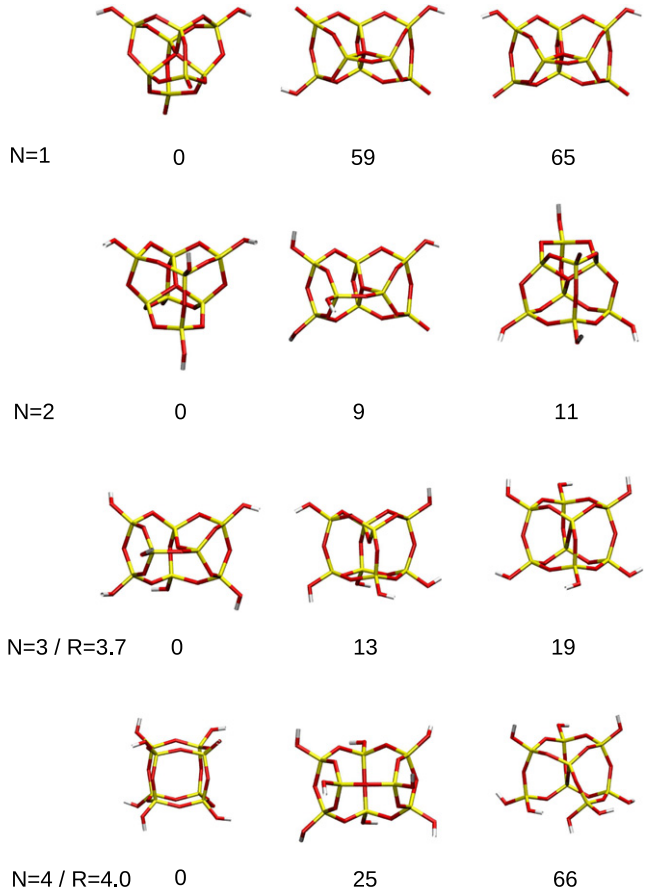

Figure 1. The three lowest energy $(SiO_2)_8(H_2O)_N$ isomer structures for different levels of hydroxylation $N = 1$, 2, 3, 4 (top to bottom). DFT energies relative to the lowest energy $(SiO_2)_8(H_2O)_N$ cluster are indicated below each geometry in kJ/mol. Yellow vertices represent silicon atoms. Red vertices represent oxygen atoms. White vertices represent hydrogen atoms. R indicates the average ring size where this could be calculated unambiguously. (For interpretation of the references to colour in this figure legend, the reader is referred to the web version of this article.)

So $\Delta_h E$ is the energy associated with the hydroxylation reaction, starting from the anhydrous (i.e. pure silica) cluster and adding N H_2O molecules.

$$(SiO_2)_M + N \cdot H_2O \rightarrow (SiO_2)_M(H_2O)_N \tag{4}$$

The anhydrous silica clusters for $M = 8$, 16 were reported in previous work [1,2] and are shown in Figure 3. $\Delta_h E < 0$ means that a hydroxylation reaction is energetically favourable. Figure 4 shows $\Delta_h E$ versus the level of hydroxylation, N, for both the Si_8O_{16} and the $Si_{16}O_{32}$ based clusters. In all cases we have $\Delta_h E < 0$. Furthermore, $\Delta_h E$ is decreasing monotonically with N (i.e. becoming more negative), meaning that *all* hydroxylation reactions

$$(SiO_2)_M(H_2O)_{N_1} + N_2 \cdot H_2O \rightarrow (SiO_2)_M(H_2O)_{N_1+N_2} \tag{5}$$

(with $N_1 + N_2 \leqslant 4$) are energetically downhill. More specifically, the addition of a single H_2O can be considered:

$$(SiO_2)_M(H_2O)_{N-1} + H_2O \rightarrow (SiO_2)_M(H_2O)_N \tag{6}$$

The associated change in energy is given by

$$\Delta_h^1 E = E_{M,N} - E_{M,N-1} - E(H_2O) \tag{7}$$

This decrement of the energy is plotted in Figure 5.

The energetic trend shows saturation in the sense that, as the degree of hydroxylation increases, the reduction in energy through the addition of another H_2O becomes less. This can be seen most

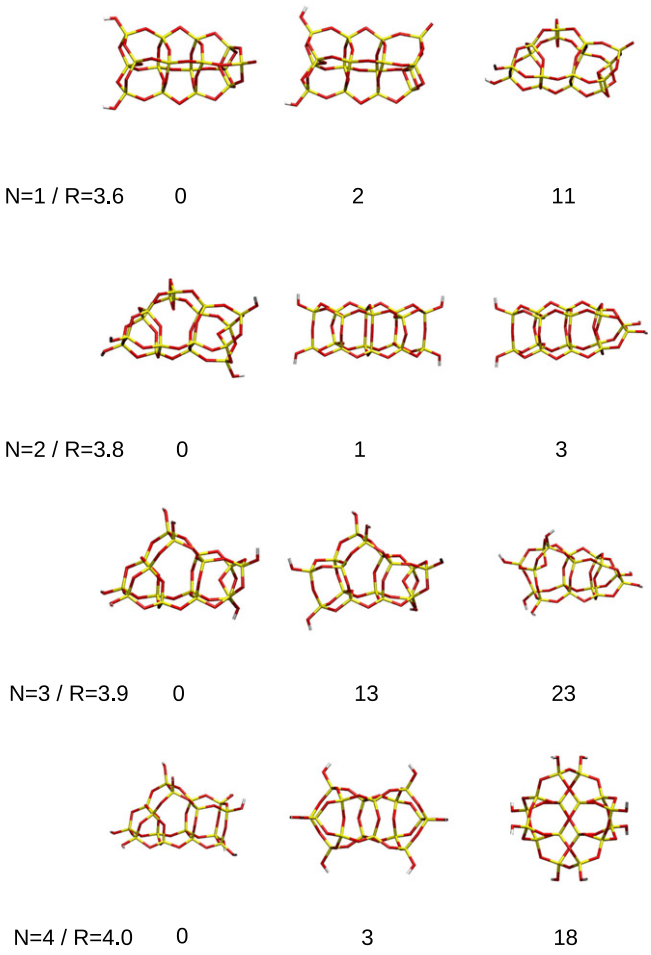

Figure 2. The three lowest energy $(SiO_2)_{16}(H_2O)_N$ geometries (left to right) for different levels of hydroxylation $N = 1, 2, 3, 4$ (top to bottom). DFT energies relative to the lowest energy $(SiO_2)_{16}(H_2O)_N$ cluster are indicated below each geometry in kJ/mol. R indicates the average ring size.

Table 1
Comparison of DFT and empirical potential energetic ordering for $(SiO_2)_M(H_2O)_N$ minima for $M = 8, 16$ and for varying levels of hydroxylation $N = 1, 2, 3, 4$. The entries in the columns labelled 1, 2, 3 indicate where the clusters that are lowest, second lowest and third lowest in DFT energy are placed in the ordering according to the empirical potential.

M	N	1	2	3	M	N	1	2	3
8	1	1	6	3	16	1	1	2	12
8	2	1	4	2	16	2	6	4	3
8	3	3	2	1	16	3	3	5	2
8	4	1	2	5	16	4	7	2	1

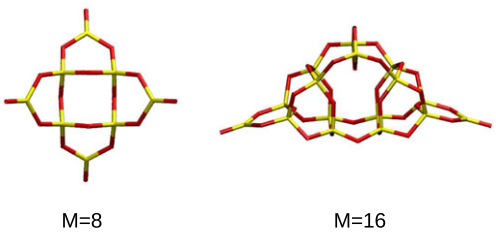

Figure 3. Candidate global minima with respect to the DFT calculated energy for pure (non-hydroxylated) silica clusters: $(SiO_2)_8$ and $(SiO_2)_{16}$.

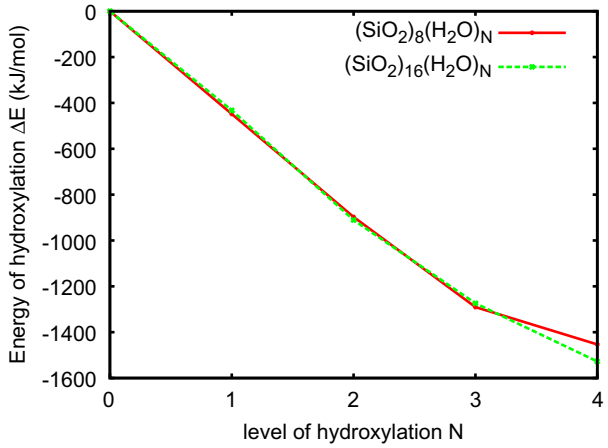

Figure 4. Energies of hydroxylation $\Delta_h E$, defined in Eq. (3), of $(SiO_2)_8(H_2O)_N$ geometries (red line) and $(SiO_2)_{16}(H_2O)_N$ geometries (green line) versus level of hydroxylation $N = 0, 1, 2, 3, 4$. (For interpretation of the references to colour in this figure legend, the reader is referred to the web version of this article.)

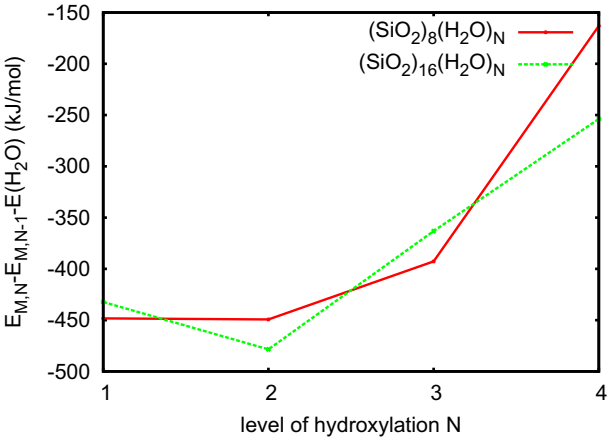

Figure 5. Decrements of the total energy $\Delta_h^1 E = E_{M,N} - E_{M,N-1} - E(H_2O)$ for $(SiO_2)_8(H_2O)_N$ geometries (red line) and $(SiO_2)_{16}(H_2O)_N$ geometries (green line) versus level of hydroxylation $N = 1, 2, 3, 4$. (For interpretation of the references to colour in this figure legend, the reader is referred to the web version of this article.)

easily from the plot of the decrements $\Delta_h^1 E$ of the energy in Figure 5. We note that the hydroxylation energy for water addition to the $(SiO_2)_{16}(H_2O)$ cluster appears to be particularly energetically favourable (i.e. even more than that for the initial hydroxylation of the anhydrous $(SiO_2)_{16}$ cluster). We suggest that this may be related to the change in structural topology of the ground state in going from $N = 1$ to $N = 2$, see Figure 2.

The $M = 8$ and $M = 16$ data can be combined to study 'condensation' reactions, where two $M = 8$ clusters react to form an $M = 16$ cluster:

$$(SiO_2)_8(H_2O)_{N_1} + (SiO_2)_8(H_2O)_{N_2} \rightarrow (SiO_2)_{16}(H_2O)_{N_1+N_2} \quad (8)$$

Note that the level of hydroxylation of the resulting $M = 16$ cluster is the sum of the levels of hydroxylation N_1, N_2 of the reacting $M = 8$ clusters. The change of energy due to this reaction is given by:

$$\Delta_c E = E_{16,N_1+N_2} - (E_{8,N_1} + E_{8,N_2}) \quad (9)$$

These reaction energies $\Delta_c E$ are tabulated in Table 2. With the current data-set condensation reaction energies with $N_1 + N_2 \leqslant 4$ can be calculated. All these reactions are energetically downhill showing that hydroxylation does not hinder the favourable energetics of cluster growth. Although there are no obvious trends in this relatively small set of energies, we note that the largest and smallest

Table 2
Left: energy $\Delta_c E$ (defined in Eq. (9)) associated with the condensation reaction (8) where two $M = 8$ clusters react to form an $M = 16$ cluster. N_1 and N_2 represent the levels of hydroxylation of the reactants. $N_1 + N_2$ is the level of hydroxylation of the product. Right: formation energy $\Delta_f E_{M,N}$ (defined in Eq. (11)) for $M = 8$, 16 and $N = 0$, 1, 2, 3, 4.

N_1	N_2	$N_1 + N_2$	$\Delta_c E$ (kJ/mol)	N	$\Delta_f E_{8,N}$ (kJ/mol)	$\Delta_f E_{16,N}$ (kJ/mol)
0	0	0	−1127	0	1482	1837
0	1	1	−1111	1	1034	1405
0	2	2	−1140	2	584	927
0	3	3	−1110	3	192	563
0	4	4	−1201	4	29	310
1	1	2	−1141			
1	2	3	−1055			
1	3	4	−916			
2	2	4	−859			

condensation energy are found for the $N = 4$ $(SiO_2)_{16}$ cluster product. The largest condensation energy is for the reaction between the fully hydroxylated ($N = 4$) $(SiO_2)_8$ ground state cluster and the anhydrous ($N = 0$) $(SiO_2)_8$ ground state cluster. Conversely, the smallest condensation energy is for a coalescing pair of $N = 2$ $(SiO_2)_8$ clusters.

Another important reaction is the formation of the cluster from fully hydroxylated monomers $Si(OH)_4$:

$$M \cdot Si(OH)_4 \rightarrow (SiO_2)_M(H_2O)_N + (2M - N) \cdot H_2O \quad (10)$$

and the associated change in energy is given by:

$$\Delta_f E_{M,N} = E_{M,N} + (2M - N) \cdot E(H_2O) - M \cdot E(Si(OH)_4) \quad (11)$$

The formation energy $\Delta_f E_{M,N}$ with respect to $Si(OH)_4$ monomers is tabulated in Table 2 for $M = 8$,16 and $N = 0$, 1, 2, 3, 4. Note that these energies are all positive meaning that the formation of our clusters in gas phase from small hydroxylated Si species is energetically unfavourable. Apparently, for the range of N considered, the energetic benefit of this type of silica condensation is outweighed by the energetic cost of dehydroxylation (i.e. releasing water molecules). Considering such reactions beyond the bare enthalpic contribution, the free energy cost is likely to be lower in each reaction due to the entropy-increasing effect of the relatively large number of product water molecules created. In addition, if occurring in solution, the full free energy balance of the reactions would also have to take into account the potentially large effects of solvation. Even in gas phase we note that our bare energy of formation is particularly low for the $(SiO_2)_8(H_2O)_4$ cubic ground state.

In addition to energetics we can also analyse the changes in structure with increasing hydroxylation. In silica-based clusters many of the silicon atoms are 4-fold coordinated by oxygen atoms. It is a well-known fact that such silicon centres prefer to be tetrahedral, i.e. the preferred O–Si–O angle is the ideal tetrahedral angle $\alpha = \arccos(-1/3) = 109.47°$. Distortion of the O–Si–O angles (away from the ideal angle) generally leads to an increase in energy. Figure 6 shows a measure of the deviation from tetrahedrality plotted against the level of hydroxylation. This tetrahedral distortion is calculated from the squared deviation of the O–Si–O angle from the ideal angle, averaged over all six angles associated with a 4-fold coordinated silicon atom and averaged over all such silicon atoms in the cluster (all angles being measured in degrees). As a general trend, the silicon centres become more tetrahedral as the degree of hydroxylation progresses. However, the first hydroxylation step, starting from a bare silica cluster and adding a single H_2O unit, does not follow this trend, especially for the Si_8O_{16} based clusters. This is probably related to the 'magic' nature of the bare Si_8O_{16} cluster: it has an anomalously low energy and an anomalously low deviation from tetrahedrality. Furthermore, this cluster has a lot of 3-fold coordinated silicon atoms, which are not taken into account in our measure, thus resulting in an anomalously low value.

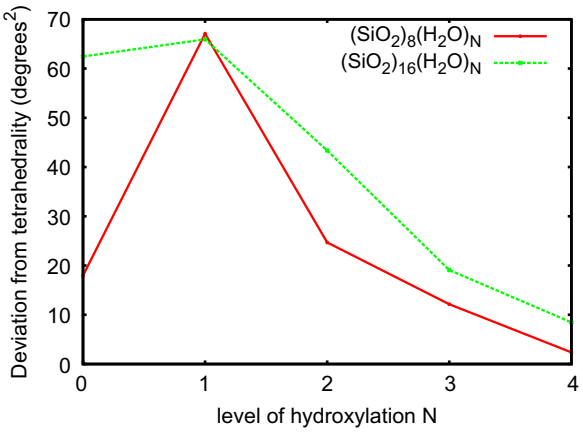

Figure 6. Average squared deviation of the O–Si–O angle from the ideal tetrahedral angle ($\alpha = 109.47°$) versus the level of hydroxylation $N = 0$, 1, 2, 3, 4. The red line corresponds to $(SiO_2)_8(H_2O)_N$ clusters. The green line corresponds to $(SiO_2)_{16}(H_2O)_N$ clusters. (For interpretation of the references to colour in this figure legend, the reader is referred to the web version of this article.)

For those clusters where the atom connectivity allows we have also computed the average $(SiO)_x$ fundamental ring [29] size (where $R = \bar{x}$), see Figures 1 and 2. Probably due to geometric restrictions, we find that, for any fixed (M, N) pair, R is the same (at least to the accuracy reported) for all three reported lowest energy isomers-thus explaining why only a single value is shown for each N value in Figures 1 and 2. In line with the $N = 1 - 4$ decrease in tetrahedral distortion noted above, the average ring size in the clusters also increases with increasing hydroxylation, also implying a opening up of the cluster structures with higher N values. This trend is most clearly seen for the $M = 16$ cluster series where R could be computed for all clusters. From the limited data obtainable from the $M = 8$ clusters it appears that this trend is also more gradual for the larger $M = 16$ clusters. Of interest, however, is the fact that R coincides at a value of exactly 4 for both the $M = 8$ and $M = 16$ clusters for $N = 4$.

The low energy set of $(SiO_2)_8$-based clusters predominantly display two types of structures which can roughly be described as: triangular prismatic (e.g. ground state for $(SiO_2)_8(H_2O)_3$) or cubic (e.g. ground states for $(SiO_2)_8(H_2O)_N$, $N = 1$, 2, 4), see Figure 1. We note that these rather compact structure types are both quite different from the more open anhydrous $(SiO_2)_8$ ground state, see Figure 3. The largest energy difference between a ground state and the second lowest energy isomer (59 kJ/mol) is found for $(SiO_2)_8(H_2O)$, which has been ascribed as a contributing reason for the experimental observation of magic deprotonated cluster anions based on this composition [9,10]. It is also noted that at the highest degree of hydroxylation considered the cubic $(SiO_2)_8(H_2O)_4$ isomer with a single hydroxyl group attached to every silicon centre is lowest in energy and separated from the next lowest energy isomer by 25 kJ/mol. This cluster is also known as a double four-ring and has been experimentally observed and has potential relevance to zeolite synthesis [12–14].

The $(SiO_2)_{16}$-based clusters tend to have much smaller energy gaps between the ground state and the next lowest energy isomer (in all cases $\leqslant$13 kJ/mol), see Figure 2. Although for the lowest level of hydroxylation a cubic columnar structure appears to be the ground state, for higher hydroxylations an isomer type based on a conjunction of a triangular prism, a pentagonal prism and a cube dominates. Unlike in the case of the $(SiO_2)_8$-based clusters, this type of structure is quite reminiscent of the anhydrous $(SiO_2)_{16}$ ground state, see Figure 3. This finding suggests that larger clusters of anhydrous silica may be more robust with respect to maintaining their internal structural topology upon hydroxylation.

Although this proposal may be reasonable to expect based on the number of surface atoms relative to bulk-like atoms, and thus the percentage of a cluster's atoms that would be involved in hydroxylation, it has been observed that hydroxylation can totally change the internal structure of considerably larger clusters of other inorganic materials [30]. To investigate this phenomenon more generally for nanoparticulate silica we are currently investigating the effects of hydroxylation on larger silica clusters [31].

4. Conclusions

We report the low energy isomer spectrum of eight different gas phase hydroxylated silica cluster compositions representing the initial stages of hydration of $(SiO_2)_M$ $M = 8$, 16 anhydrous silica clusters. Using a computationally efficient empirical potential representation of the PES, we employ basin hopping global optimisation and subsequent DFT refinement to obtain our set of isomers. The empirical potential employed is found to perform satisfactorily with respect to its predicted energetic ordering of isomers compared to the corresponding DFT calculated energetic ordering. Incremental hydroxylation of the respective anhydrous silica ground states is found to always be favourable but less so with increasing addition of water. Condensation reactions between pairs of $(SiO_2)_8(H_2O)_N$ clusters to form $(SiO_2)_{16}(H_2O)_{N'}$ are also all energetically favourable. $(SiO_2)_8$-based and $(SiO_2)_{16}$-based clusters also both tend to become more tetrahedral with respect to their SiO_4 centres and to have larger average $(SiO)_x$ ring sizes with increasing hydroxylation. Hydroxylation is also found to affect the overall structural topology of the smaller cluster set more than for the larger clusters considered.

Acknowledgments

Edwin Flikkema holds a RCUK Academic Fellowship. Kim E. Jelfs acknowledges support from HPC-EUROPA2. This study has further been supported by the Spanish Ministry of Science and Innovation MICINN (Grant FIS2008-02238) and by the Generalitat de Catalunya (Grants 2009SGR1041 and XRQTC).

References

[1] E. Flikkema, S.T. Bromley, J. Phys. Chem. B 108 (28) (2004) 9638.
[2] S.T. Bromley, E. Flikkema, Phys. Rev. Lett. 95 (2005) 185505.
[3] E. Flikkema, S.T. Bromley, Phys. Rev. B 80 (2009) 035402.
[4] J.C.G. Pereira, C.R.A. Catlow, G.D. Price, J. Phys. Chem. A 103 (1999) 3268.
[5] M.J. Mora-Fonz, C.R.A. Catlow, D.W. Lewis, J. Phys. Chem. C 111 (2007) 18155.
[6] T.T. Trinh, A.P. Jansen, R.A. van Santen, E.J. Meijer, J. Phys. Chem. C 113 (2009) 2647.
[7] C.E. White, J.L. Provis, G.J. Kearley, D.P. Riley, J.S.J. van Deventer, Dalton Trans. 40 (2011) 1348.
[8] C.L. Schaffer, K.T. Thomson, J. Phys. Chem. C 112 (2008) 12653.
[9] C. Xu, W. Wang, W. Zhang, J. Zhuang, L. Liu, Q. Kong, L. Zhao, Y. Long, K. Fan, S. Qian, Y. Li, J. Phys. Chem. A 104 (2000) 9518.
[10] S.T. Bromley, E. Flikkema, J. Chem. Phys. 122 (2005) 114303.
[11] J.C. Wojdel, M.A. Zwijnenburg, S.T. Bromley, Chem. Mater. 18 (2006) 1464.
[12] A. Aerts, C.E.A. Kirschhock, J.A. Martens, Chem. Soc. Rev. 39 (2010) 4626.
[13] C.T.G. Knight, R.J. Balec, S.D. Kinrade, Angew. Chem. Int. Ed. 46 (2007) 8148.
[14] S.A. Pelster, B. Weimann, B.B. Schaack, W. Schrader, F. Schüth, Angew. Chem. Int. Ed. 119 (2007) 6794.
[15] K.E. Jelfs, E. Flikkema, S.T. Bromley, Chem. Commun. 48 (2012) 46.
[16] S. Tsuneyuki, M. Tsukada, H. Aoki, Y. Matsui, Phys. Rev. Lett. 61 (1988) 869.
[17] B. van Beest, G. Kramer, R. van Santen, Phys. Rev. Lett. 64 (1990) 1955.
[18] E. Flikkema, S.T. Bromley, Chem. Phys. Lett. 378 (2003) 622.
[19] A. Hassanali, S. Singer, J. Phys. Chem. B 111 (2007) 11181.
[20] D.C. Liu, J. Nocedal, Math. Program. 45 (1989) 503.
[21] B. Hartke, Struct. Bond. 110 (2004) 33.
[22] C.R.A. Catlow, S.T. Bromley, S. Hamad, M. Mora-Fonz, A.A. Sokol, S.M. Woodley, Phys. Chem. Chem. Phys. 12 (2010) 786.
[23] D. Wales, J.P.K. Doye, J. Phys. Chem. A 101 (1997) 5111.
[24] S.T. Bromley, E. Flikkema, Comput. Mater. Sci. 35 (2006) 382.
[25] J.J.P. Stewart, J. Comput. Chem. 10 (1989) 209.
[26] A. Becke, J. Phys. Chem. 98 (1993) 5648.
[27] M. Guest et al., Mol. Phys. 103 (2005) 719.
[28] S. Hamad, S.T. Bromley, Chem. Commun. 35 (2008) 4156.
[29] O. Delgado-Friedrichs, M. O'Keeffe, J. Solid State Chem. 178 (2005) 2480.
[30] H. Zhang, B. Gilbert, F. Huang, J. Banfield, Nature 424 (2003) 1025.
[31] K. Jelfs, E. Flikkema, S. Bromley, in preparation.